J Mater Sci: Mater Med (2009) 20:1505–1512
DOI 10.1007/s10856-009-3713-5

In vivo study of porous strontium-doped calcium polyphosphate scaffolds for bone substitute applications

Meng Tian · Feng Chen · Wei Song · Yancheng Song · Yuanwei Chen · Changxiu Wan · Xixun Yu · Xiaohua Zhang

Received: 5 July 2008 / Accepted: 9 February 2009 / Published online: 9 March 2009

Abstract The purpose of this study was to investigate in vivo biocompatibility and osteogenesis as well as degradability of the porous strontium-doped calcium polyphosphate (SCPP) scaffolds as a biomaterial for bone substitute applications. The evaluation was performed on a rabbit model over a period of 16 weeks by histology combined with image analysis, X-ray microradiography and immunohistochemistry methods. The histological and X-ray microradiographic results showed that the SCPP scaffold exhibited good biocompatibility and extensive osteoconductivity with host bone. Moreover, a significant more bone formation was observed in the SCPP group compared with that in the CPP group, especially at the initial stage after implantation. New bone volumes (NBVs) of the SCPP group determined at week 4, 8 and 16 were 14, 27 and 45%, respectively. Accordingly, NBVs of the CPP group were 10, 19 and 40%. Immunohistochemical results revealed that both the expression of collagen type I and bone morphogenetic proteins in the SCPP group were higher than that in the CPP group, which might be associated with the release of strontium ions during the implantation. In addition, during 16 weeks implantation the SCPP scaffold exhibited similar degradability with the CPP scaffold in vivo. Both scaffolds showed the greatest degradation rate for the first 4 weeks, and then the degradation rate gradually decreased. The results presented in this study demonstrated that SCPP scaffold can be considered as a biocompatible material, making it attractive for bone substitute application purposes.

M. Tian · F. Chen · W. Song · Y. Chen · C. Wan (✉) · X. Yu · X. Zhang
Department of Biomedical Polymers and Artificial Organs, College of Polymer Science and Engineering, Sichuan University, Chengdu, Sichuan 610065, China
e-mail: wanchangxiu@163.com

Y. Song
Department of Orthopaedics, West China Hospital, Sichuan University, Chengdu, Sichuan 610041, China

1 Introduction

Developmental pathology, accidents, and tumor resection frequently cause bone loss, which still is a problem in orthopedic and reconstructive surgery. To resolve these problems, many types of bone substitutes have been developed [1]. Calcium polyphosphate (CPP), a kind of calcium phosphates, has drawn more and more attention in recent due to its similar chemical elements to bones and the degradability in biological environments. There have been some reports on the possible use of CPP in the literature [2–4]. These studies suggested the potential of CPP as a bone substitute material.

On the other hand, strontium (Sr) has been gradually recognized during the research of treatment for osteoporosis. It enhances the replication of bone cells, and simulates bone formation in calvarial cultures in vitro [5]. Furthermore, it has been demonstrated that strontium ranelate decreased bone resorption in vivo [6, 7]. The resulting increase in bone mineral density seems to be associated with improved mechanical properties of bone. As a kind of bone-seeking trace elements, Sr has various effects on bone metabolism depending on the dose used. At low dose levels, stable Sr is of great benefit to bone formation as mentioned above. However, high doses of Sr can induce bone changes in experimental animals, especially if calcium (Ca) intake is low [8, 9]. This seems to be caused by a combination of impaired intestinal absorption of Ca and reduced renal production of 1,25-dihydroxy cholecalciferol.

In our previous study, a novel strontium-doped calcium polyphosphate (SCPP) scaffold was prepared and osteoblasts were seeded on the SCPP scaffolds to estimate the optimal dose of Sr [10].The results indicated that a dose of 1% Sr was optimal. In this work, in vivo biocompatibility and osteogenesis as well as degradability of the porous SCPP scaffolds was investigated in a rabbit model, in order to demonstrate potential bone substitute applications of this material.

2 Materials and methods

2.1 Preparation and characterization of the scaffolds

The SCPP scaffold was prepared according to a procedure described previously [10, 11]. The CPP scaffold was prepared under the same conditions and served as a control. The resulting scaffolds were 4 mm in diameter and 15 mm in thickness. Microstructure of the scaffolds was characterized by scanning electron microscope (SEM; JSM-5900LV, JEOL Techniques, Tokyo, Japan) and X-ray diffraction (XRD; X' Pert Pro MPD, Philips, Netherlands).

2.2 Animal experiments

In vivo evaluation was performed by implanting the scaffolds in rabbit left foreleg radiuses. The scaffolds without adding any growth factor or living cell were used to repair 15 mm segmental defects in the implantation experiment. Forty eight healthy New Zealand white rabbits weighting about 2.5 ± 0.4 kg each were divided into two groups, one for implantation of the SCPP scaffolds, another for the CPP scaffolds. With the animal under general anesthesia, the diaphysis of its radius was exposed through a longitudinal extensile incision, and then a 15 mm segmental bony defect was inflicted. The defect was filled with the prepared scaffold, and the wound was closed.

2.3 Histology and microradiography

For histological study, six rabbits from each group were sacrificed at 4, 8 and 16 weeks respectively after implantation. The scaffolds together with surrounding tissue were excised, fixed in 4% paraformaldehyde, decalcified in 10% EDTA and embedded in paraffin. The embedded tissue blocks were sectioned at 5 μm in thickness and stained with hematoxylin and eosin (H&E). Histological sections were observed by light microscope (BX41, Olympus, Japan). To monitor the bone formation as closely as possible, some rabbits were examined using X-ray microradiography before histological study at 16 weeks.

2.4 Quantification of newly formed bone and residual material

Quantitative determinations of newly formed bone and residual material were performed using image and statistical analysis of histological sections. In every implantation time, six pieces of histological sections were randomly chosen from both SCPP and CPP groups. After H&E stained, each section was observed under light microscope with 50× magnification, and at least 10 images were randomly obtained in one section. Using image analytical software Image-ProPlus (Media Cybernetics, USA), new bone volume (NBV) was expressed as the percentage of newly formed bone area in the available pore space (bone area/pore area × 100%), and residual material volume (RMV) was expressed as the percentage of scaffold material area in the total implant area (scaffold material area/total implant area × 100%).

2.5 Immunohistochemistry

For immunohistochemical study, six rabbits from each group were sacrificed at 2 weeks respectively after implantation. The scaffolds together with surrounding tissue were excised, fixed in 4% paraformaldehyde, and then decalcified in 10% EDTA. After being dehydrated in graded alcohol and embedded in paraffin, tissue blocks were sectioned at 5 μm in thickness and then used for collagen type I (COL I) immunohistochemical staining and bone morphogenetic proteins (BMP)-2 immunohistochemical staining. When collagen type I immunohistochemical staining was employed, the sections were immersed in 3% hydrogen peroxide for 10 min and then blocked with 10% normal goat serum in PBS at room temperature for 30 min. Next, the sections were incubated with monoclonal rat anti-human COL I antibody (Santa Cruz, USA) diluted in PBS in humidified boxes for 60 min at 37°C, then incubated with biotin-marked goat anti-mouse immunoglobulin G (Beijing Zhongshan Biotech Co., Ltd., China) for 20 min at 37°C and horseradish-marked streptomycin avidin (Beijing Zhongshan Biotech Co., Ltd., China) for 20 min at 37°C. After DAB coloration and hematoxylin staining, the sections were washed with PBS, coverslipped and viewed with a light microscope. A negative control was prepared by omitting the primary antibody. For BMP-2 immunohistochemical staining, the sections were quenched with 3% hydrogen peroxide for 20 min and digested with 0.05% trypsin for 20 min at 37°C then blocked with 10% normal goat serum in PBS at room temperature for 30 min to block endogenous peroxidase and non-specific protein binding, respectively. The sections were incubated with a primary antibody, in which monoclonal rat anti-rabbit BMP-2 antibody (Santa Cruz, CA) was diluted in PBS in

humidified boxes for 60 min at 37°C. The following operations were according to the above steps. The mean deepness values (gray-scale value) of immunohistochemical staining of COL I and BMP-2 were quantitative determined with LeicaQuantimet 500 Image analyzer (Wetzlar, Germany). Six pieces of the sections were randomly chosen from both SCPP and CPP groups, and at least 10 images were randomly obtained in one section.

2.6 Statistical analysis

Statistical analysis was performed with SPSS (v12.0). Quantitative data were presented as means ± standard deviation (SD). A student's t-test was performed to determine the statistical significance between experimental groups. A value of $P < 0.05$ was considered to be statistically significant.

3 Results and discussions

3.1 Scaffold characterization

As shown in Fig. 1, both SCPP and CPP scaffolds exhibited three-dimensionally interconnected pore structure and with a pore size of about 100–400 μm. The porosity value of the scaffolds was measured by liquid displacement. The measured porosity value was about 65% for both scaffolds. For bone substitute applications, ideal scaffolds should have appropriate pore structure, pore size and porosity, to ensure a biological environment conducive to cell attachment, proliferation and flow transport of nutrients and metabolic waste. The pore size should be large enough to support cell migration and bone ingrowth against being covered by the cells, forming pore bridging and occlusion. The optimal pore size required for bone ingrowth has been suggested in the range of 100–800 μm [12]. Therefore, the three-dimensional and highly interconnected macroporous network of the prepared scaffold allows not only for cell growth and spatially even distribution but also for flow transport of nutrients and metabolic waste. The difference between the two scaffolds was that the crystal grain size of SCPP was larger than that of the CPP (Fig. 1c, f), which might be associated with the doped of Sr elements. Moreover, it seems that the crystal grains of SCPP are more intimately connected with each other, resulting in a smoother surface and a more compact bulk.

Figure 2 was the XRD patterns of SCPP and CPP scaffolds. From the patterns, it can be seen that there was no significantly difference between the two patterns of scaffolds, indicating doped Sr elements entering CPP's crystal without changing on its original structure. Compared with standard PDF card 77-1953, it was shown that characteristic peaks in each curve accorded with the standard curves, especially three characteristic calcium phosphate peaks between 20° and 30°, which indicated the crystal system of SCPP was the same as β-CPP, which was monoclinic.

3.2 In vivo studies

In implantation experiment, all surgeries on the rabbits were completed successfully and the animals survived during the 16 postoperative weeks. None of the implanted sites of the rabbits showed any infection and inflammation after the operation. Figure 3 shows optical images of H&E histological staining of the SCPP and CPP scaffolds after implantation. Both tissue response and degradation within and surrounding the scaffold could be observed. There was no adverse tissue reaction in any of the sections examined at the various time points. At 4 weeks of implantation, all the scaffolds, both in the SCPP and CPP groups, were

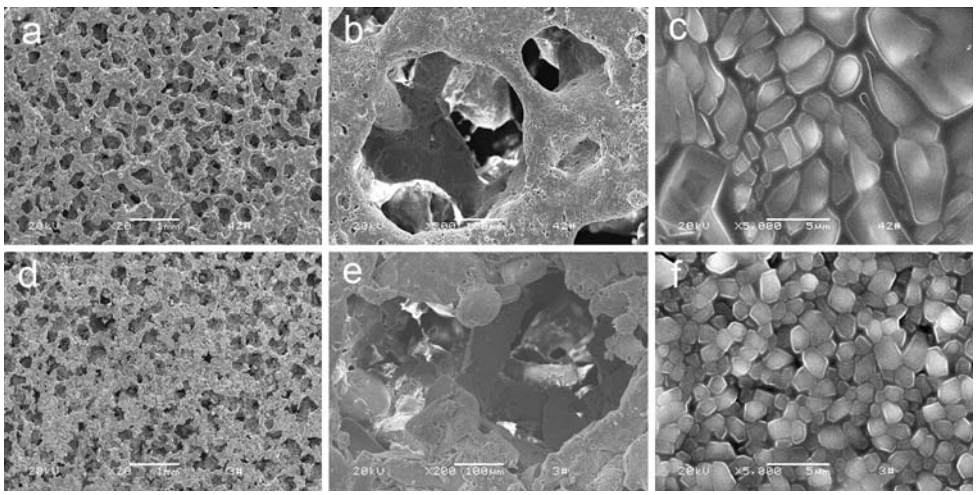

Fig. 1 SEM images of SCPP and CPP scaffolds (SCPP: **a** 20×, **b** 200×, **c** 5000×; CPP: **d** 20×, **e** 200× and **f** 5000×)

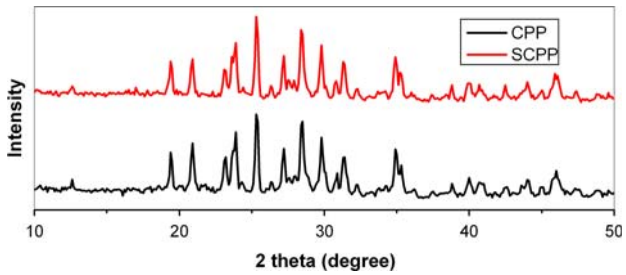

Fig. 2 XRD patterns of SCPP and CPP scaffolds

encapsulated by fibrous collagen, and the interface between scaffold and natural bone was clearly visible. New bone was observed in the margins of the implant, and there was no new bone formation in the center of the scaffolds (Fig. 3c). In the SCPP group, an active bone formation, which was evident by large number of osteoblasts and osteocytes, was seen in Fig. 3a. These osteoblasts were found lining the front-line of the developing bone and the osteocytes in the almond-shaped lacunae were embedded randomly in the bone matrix, which indicated that new bone was mainly of the woven type. However, in the CPP group, only a small quantity of osteoblasts was observed, which was the evidence of amount of bone formation. With the implantation prolonged, more newly formed bone tissues, including bone trabecular and lacuna, were observed with the presence of active osteoblasts in the SCPP group after implantation for 8 weeks (Fig. 3d). Fibrous connective tissue was located predominantly in the intertrabecular area. Moreover, a large proportion of osteoblasts penetrated through the interconnective pores to the center of the scaffold (Fig. 3f), which would accelerate the mineralization and regeneration of new bone. In addition, degradation of the scaffold was observed, indicated by the loss of integrity of the implant and concomitant replacement by newly formed bone with increasing implantation time. In contrast, numerous osteoblasts were observed from the histological results of the CPP scaffold. Newly formed bone increased gradually both in quantity and maturation (Fig. 3e). Finally, after 16 weeks of implantation new bone regenerated and penetrated through the interconnective pores to the center of the scaffolds (Fig. 3i), increasing the quantity and density of the defected area. Fibrous tissues in the intertrabecular area were replaced by hematopoietic marrow (Fig. 3g). The interface between material and host bone was hardly detectable and formed a close union without any gap. In the case of the CPP group, new bone with trabecular structure encasing the scaffold was consistently seen (Fig. 3h). While in the center of the scaffold, it was observed no new bone but only fibrous tissues formation.

To quantitatively determine the amount of newly formed bone, we statistically analyzed the histological sections of different implantation periods. Figure 4 shows NBV at each implantation period. Obviously, before 8 weeks post-implantation, the amounts of newly formed bone in SCPP group increased dramatically, much more than that of CPP scaffold. After that period, however, bone formation in

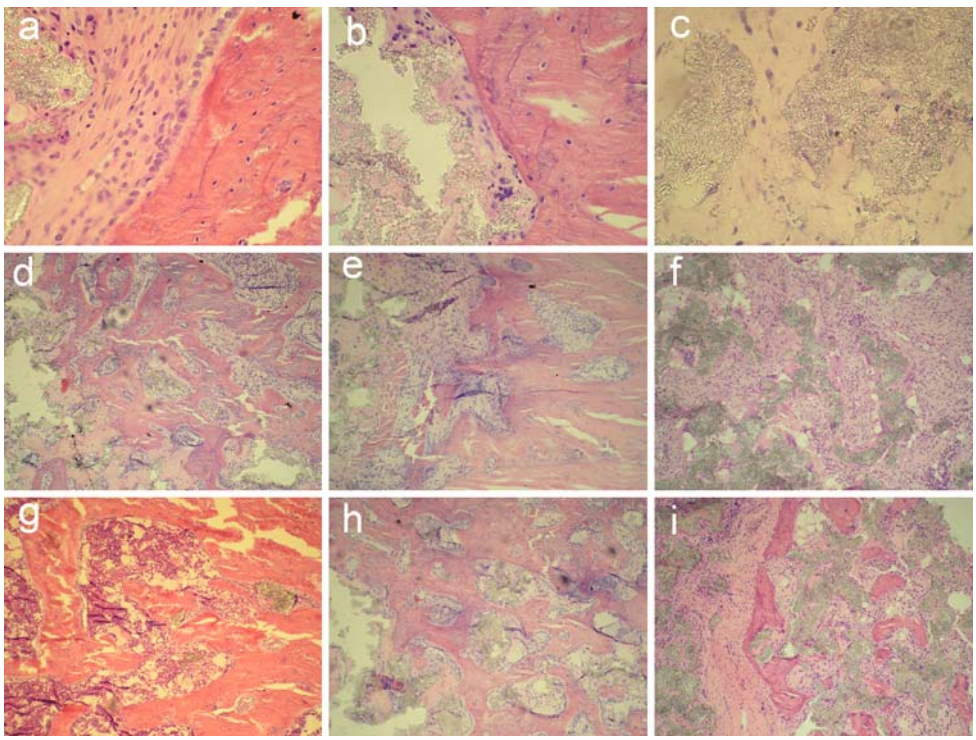

Fig. 3 Histological sections of SCPP and CPP scaffolds after 4 (**a**, **b**, **c** 200×), 8 (**d**, **e**, **f** 50×), and 16 (**g**, **h**, **i** 50×) weeks of implantation (SCPP: **a**, **c**, **d**, **f**, **g**, **i**; CPP: **b**, **e**, **h**). In the SCPP group, **c**, **f** and **i** are the center areas of the scaffolds at the various time points respectively

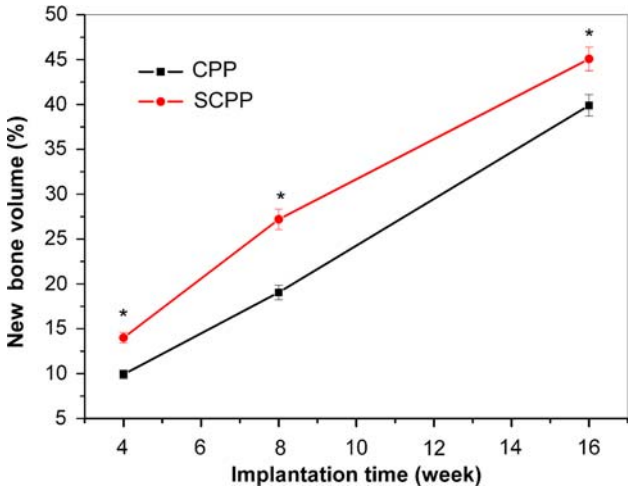

Fig. 4 Quantification of newly formed bone was performed using statistical analysis of histological sections. Error *bars* represent means ± SD for $n = 6$. $^*P < 0.05$ (compared to CPP group)

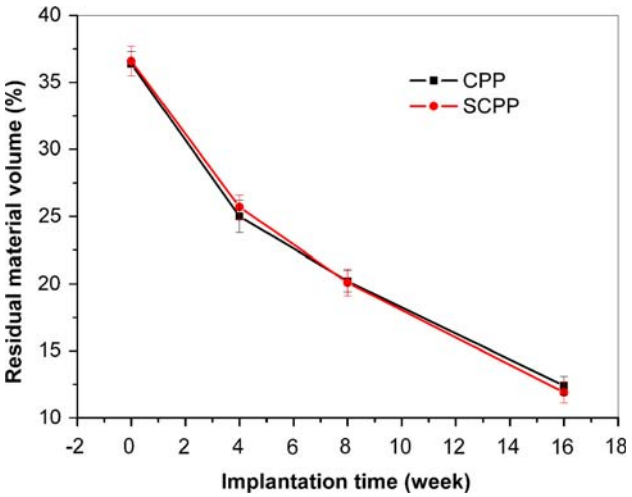

Fig. 5 Quantitative determination of residual material was performed using statistical analysis of histological sections. Error bars represent means ± SD for $n = 6$. Statistical analysis indicated there was no statistical significance at any time points

SCPP scaffold slowed down, while in CPP scaffold the speed of new bone formation gradually grew. At 16 weeks, NBVs of SCPP and CPP group were 45% and 40%, respectively. These results demonstrated that SCPP scaffolds presented higher efficiency of bone formation than CPP scaffolds at the initial stage of implantation, but in long term (>16 weeks) both scaffolds might show similar osteogenesis.

The present in vivo evaluation indicates the SCPP scaffold has good biocompatibility and osteoconductivity 16 weeks postoperation in the rabbit radiuses. The pattern of the formed new bone was similar to that reported previously in the literature with bone being formed first at the margins of the implants and then growing into the porous structure [13]. Compared with the CPP scaffolds, the enhanced bone formation of the SCPP scaffold might be associated with the release of Sr ions during the degradation process. It had been suggested that the distribution of body Sr located in bone [14] and the supplementing Sr resulted in a significant increase in bone density and bone strength [6, 7]. Moreover, it was reported that Sr could enhance bone cell replication and bone formation in vitro [5]. Therefore, the release of Sr ions in this study might have contributed to the enhanced formation of bone tissue around and within the SCPP scaffold.

During 16 weeks implantation, the percentage of residual scaffold material at all time points was shown in Fig. 5. For both scaffolds, the degradability was found to be similar and there was no statistical significance of degradation rate at any time points. The two scaffolds exhibited the greatest degradation rate for the first 4 weeks, and then the degradation rate gradually decreased. After 16 weeks implantation, the percentages of residual SCPP and CPP scaffold materials respectively were 11.9% and 12.4%, which corresponded to 67.5% and 65.9% material degradation for SCPP and CPP scaffold, respectively. In general, the degradation rate of CPP scaffold in vivo was affected by following 3 factors [3]: (1) initial size of particles from which the scaffold was formed; (2) scaffold structure, including pore size, porosity and crystal type; (3) implantation site. The above 3 factors for SCPP and CPP group were similar in our experiment, which explained why it was observed no significantly different degradation rate between the two groups. However, in our previous studies, the higher degradation rate of CPP scaffold observed in vitro in physiological saline [11]. The reasons may be that in addition to the hydrolytic degradation of the scaffold in vitro, there may be a more biologically active degradation in vivo, which may be due to cellular activity, as has been shown with other calcium phosphate ceramics [3, 15].

X-ray microradiographic analysis confirms the results of the histological study that both the SCPP and the CPP substitutes are biocompatible and osteoconductive to the host bone. At 16 weeks post-implantation, the SCPP/bone boundary became illegible, suggesting the occurrence of mineralization and increasing density of the scaffold (Fig. 6b, c). The disappearance of the boundary of material and tissue indicated that the density of newly formed bone was as high as that of host bone.

COL I and BMP-2 immunohistochemical staining of the sections were shown in Figs. 7 and 8. The brown areas stained by DAB were positive results which indicated the expression of COL I and BMP-2. COL I is considered the basic initial bone matrix protein in bone formation. During the remodelling of skeletal structures, reparative cells migrate on this matrix, and subsequently organize and remodel the matrix through cytoskeleton and matrix

Fig. 6 X-ray microradiographs of the defect area (*arrow* in **a**) of rabbit radiuses after 16 weeks of implantation (SCPP: **b**; CPP: **c**)

synthesis and degradation [16]. Therefore, expression of COL I could play an important role during osteogenesis. In both groups, the expression of COL I at 2 weeks was localized within osteoblast-like cells, some osteocytes and in the front-line of the newly formed bone-like matrix on the pore surface of the scaffold. However, compared with CPP group, the expression of COL I in SCPP group (Table 1) was higher ($P < 0.05$), which might be due to the effect of the released Sr ions on related cells, e.g. osteoblasts. This phenomenon was consistent with previous report that Sr could increase collagen synthesis without affecting matrix mineralization [17].

BMP-2 stimulates proliferation of both chondrocytes and osteoblasts and causes increased matrix production in each cell type. BMPs have also been found to induce mesenchymal stem cells differentiation to osteoblasts [16].

Table 1 The mean deepness values (gray-scale value) of immunohistochemical staining of COL I and BMP-2 of histological sections at 2 weeks

Group	*n*	COL I	BMP-2
SCPP	6	132 ± 5	115 ± 4
CPP	6	124 ± 4	107 ± 4

When looking at the immunhistochemical results of BMP-2 staining, it was shown BMP-2 expression was primarily localized in the mineralized matrix of newly formed bone on the pore surface of the scaffold. The results of the expression of BMP-2 proved to be a sufficient marker of early bone formation. In addition, it can be seen from image analytical results (Table 1) that the expression of BMP-2 in SCPP group was higher than that in CPP group ($P < 0.05$). This confirmed the results obtained by histological evaluation and bone formation determination, where a significant more bone formation was observed in SCPP group at initial stage of implantation.

Recently, Sr-containing compounds or ceramics have attracted more and more interesting in the prevention and treatment of osteoporosis. There are many reports on the beneficial effects of Sr salt or Sr-containing ceramics on bone formation [5–7, 18–22], however, the cellular mechanisms underlying the effects are not completely known. Some mechanisms have been suggested in recent years [18, 19]. First, it was found that Sr, like Ca, can activate the calcium-sensing receptor (CaSR), resulting in activation of inositol-1,4,5-trisphosphate (IP3) production and mitogen-activated protein kinase (MAPK) signaling. This suggested that Sr can activate osteoblastic cell replication through the CaSR. The second mechanism is Sr can activate extracellular signal-regulated kinase (ERK) 1/2 phosphorylation, indicating that, in addition to the calcium-sensing receptor, another receptor could mediate the effect of Sr on osteoblastic cell replication. The third is that Sr may inhibit bone resorption by increasing osteoprotegerin (OPG) and decreasing receptor activator of nuclear factor kappa B ligand (RANKL) expression by osteoblasts. For the SCPP scaffold, further studies on the cellular mechanisms are carrying out in our group.

Although Sr has beneficial effects on bone formation, the possible negative effects of Sr should be also concerned, especially in a high dose of Sr. In vitro studies have indicated that Sr has a dose-dependent effect on osteoblasts [23]. At 0.5 and 1 μg/ml Sr concentration in the culture medium, a reduced intracellular nodule formation was found (impaired in vitro osteoblast differentiation), at 2–5 μg/ml nodule formation and mineralisation were normal, and at 20–100 μg/ml there was an inhibitory effect on mineralisation (reduced hydroxyapatite formation). On the other hand, in vivo studies have suggested that excessive doses of Sr could disturb the Ca metabolism. Morohashi et al. [8] investigated the effect of varying oral doses of Sr in rats. They found at constant Ca levels in the diet a significant increase in the Ca content of bones if the animals received 87.5 μmol/day Sr concentrations, but at a dose of 875 μmol/day resulted in reduced bone Ca content and hypocalcaemia. Grynpas and Marie [9] studied the effects of doses of Sr on bone quality and quantity in rats

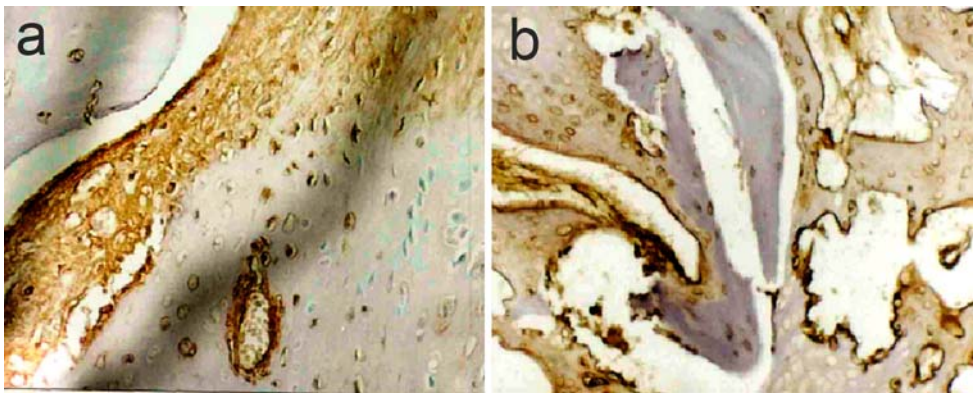

Fig. 7 COL I immunohistochemical staining of histological sections at 2 weeks (SCPP: **a**; CPP: **b**)

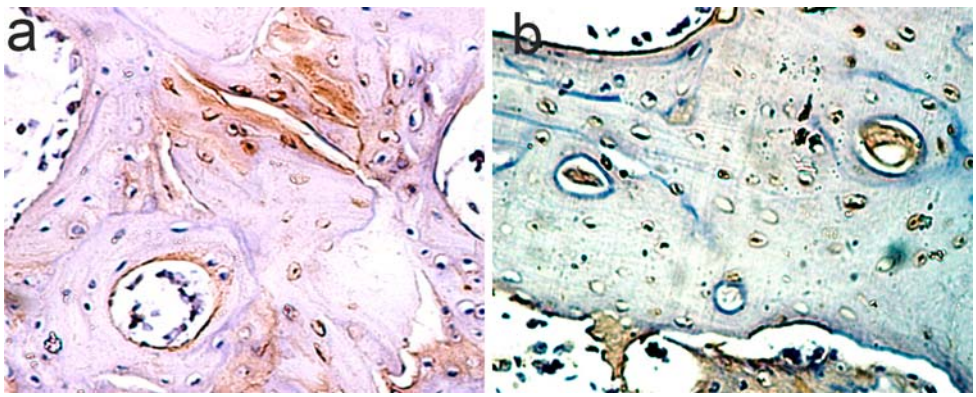

Fig. 8 BMP-2 immunohistochemical staining of histological sections at 2 weeks (SCPP: **a**; CPP: **b**)

fed a relatively low Ca diet. The results showed that Sr, in low doses, stimulated bone formation, but high doses had deleterious effects on bone mineralization. It was should be noted that the above in vivo studies were performed in rats by oral administration and the negative effects occurred in relative low Ca/Sr, that is to say, the negative effects seemed to be caused by a combination of impaired intestinal absorption of Ca and reduced renal production of 1,25-dihydroxy cholecalciferol [24]. The direct effects of Sr on intestinal Ca absorption seem to be caused by the fact that the two metals share a common absorption pathway, combined active and passive transport mechanisms favouring Ca absorption. The competitive inhibition has been demonstrated in both isolated intestinal slices and perfused intestines. In the case of direct implantation of Sr-containing ceramics, Leong et al. [20–22, 25] reported a strontium-containing hydroxyapatite (Sr-HA) bioactive cement containing 10% Sr for bone repair in recent years. Both in vitro and in vivo studies showed the cement was biocompatible and osteoconductive. There are also some other reports on Sr-containing or Sr-substituted ceramics for bone replacement, but the reports limited in structure characterization or physical performances [26, 27]. In our previous study, the effects of SCPP on osteoblast were evaluated by MTT (3-(4,5-dimethylthiazol-2yl)-2,5-diphenyltetrazolium bromide) and ALP (alkaline phosphatase) activity assay [10]. The results showed that the proliferation and ALP expression of the cells on the SCPP containing a low dose (<10%) of Sr showed a higher level compared to the control, and the SCPP containing 1% Sr was optimal. In this work, it was demonstrated that the SCPP containing 1% Sr exhibited good biocompatibility, enhanced osteogenesis and degradability in vivo. The in vitro and in vivo studies indicated that, at a dose of 1% Sr, the SCPP appeared to be safety in the experiments. However, there may be remain some unknown and delayed negative effects on body when direct implantation of the Sr-containing ceramics. For this reason, more attention needs to be paid to investigate the potential negative effects of the Sr-containing ceramics.

4 Conclusions

In this work, microstructure of SCPP scaffold was characterized by SEM and XRD measurements. Subsequently, a rabbit model was employed for in vivo study of the SCPP scaffold. The evaluation methods included histology combined with image analysis, X-ray microradiography and immunohistochemistry. The results showed that the scaffold presented good biocompatibility, enhanced osteogenesis and degradability, suggesting that the porous SCPP

material represents an acceptable bone substitute implant. In addition, the possible negative effects of strontium have been discussed.

Acknowledgements This work is supported by the National Science Foundation of China (Project No. 30870614 and 50472091).The authors would like to thank Ms. Suilin Liu and Mr. Zhu Li, researchers at the Analytical &Testing Center of Sichuan University, for valuable suggestion and specimen characterization.

References

1. Damien CJ, Parsons JR. Bone-graft and bone-graft substitutes—a review of current technology and applications. J Appl Biomater. 1991;2:187–208. doi:10.1002/jab.770020307.
2. Pilliar RM, Filiaggi MJ, Wells JD, et al. Porous calcium polyphosphate scaffolds for bone substitute applications—in vitro characterization. Biomaterials. 2001;22:963–72. doi:10.1016/S0142-9612(00)00261-1.
3. Grynpas MD, Pilliar RM, Kandel RA, et al. Porous calcium polyphosphate scaffolds for bone substitute applications in vivo studies. Biomaterials. 2002;23:2063–70. doi:10.1016/S0142-9612(01)00336-2.
4. Lee YM, Seol YJ, Lim YT, et al. Tissue-engineered growth of bone by marrow cell transplantation using porous calcium metaphosphate matrices. J Biomed Mater Res. 2001;54:216–23. doi:10.1002/1097-4636(200102)54:2<216::AID-JBM8>3.0.CO;2-C
5. Canalis E, Hott M, Deloffre P, et al. The divalent strontium salt S12911 enhances bone cell replication and bone formation in vitro. Bone. 1996;18:517–23. doi:10.1016/8756-3282(96)00080-4.
6. Buehler J, Chappuis P, Saffar JL, et al. Strontium ranelate inhibits bone resorption while maintaining bone formation in alveolar bone in monkeys (*Macaca fascicularis*). Bone. 2001;29:176–9. doi:10.1016/S8756-3282(01)00484-7.
7. Hott M, Deloffre P, Tsouderos Y, et al. S12911-2 reduces bone loss induced by short-term immobilization in rats. Bone. 2003;33:115–23. doi:10.1016/S8756-3282(03)00115-7.
8. Morohashi T, Sano T, Yamada S. Effects of strontium on calcium metabolism in rats i. a distinction between the pharmacological and toxic doses. Jpn J Pharmacol. 1994;64:155–62. doi:10.1254/jjp.64.155.
9. Grynpas MD, Marie PJ. Effects of low doses of strontium on bone quality and quantity in rats. Bone. 1990;11:313–9. doi:10.1016/8756-3282(90)90086-E.
10. Qiu K, Zhao XJ, Wan CX, et al. Effect of strontium ions on the growth of ROS17/2.8 cells on porous calcium polyphosphate scaffolds. Biomaterials. 2006;27:1277–86. doi:10.1016/j.biomaterials.2005.08.006.
11. Chen YW, Shi GQ, Ding YL, et al. J Mater Sci Mater Med. 2008;19:2655–62. doi:10.1007/s10856-007-3350-9.
12. Sous M, Bareille R, Rouais F, et al. Cellular biocompatibility and resistance to compression of macroporous beta-tricalcium phosphate ceramics. Biomaterials. 1998;19:2147–53. doi:10.1016/S0142-9612(98)00118-5.
13. Merkx MAW, Maltha JC, Freihofer HM, et al. Incorporation of three types of bone block implants in the facial skeleton. Biomaterials. 1999;20:639–45. doi:10.1016/S0142-9612(98)00219-1.
14. Dahl SG, Allan P, Marie PJ, et al. Incorporation and distribution of strontium in bone. Bone. 2001;28:446–53. doi:10.1016/S8756-3282(01)00419-7.
15. Yamada S, Heymann D, Bouler JM, et al. Osteoclastic resorption of calcium phosphate ceramics with different hydroxyapatite beta-tricalcium phosphate ratios. Biomaterials. 1997;18:1037–41. doi:10.1016/S0142-9612(97)00036-7.
16. Thorwartha M, Rupprechta S, Falkb S, et al. Expression of bone matrix proteins during de novo bone formation using a bovine collagen and platelet-rich plasma (prp)—an immunohistochemical analysis. Biomaterials. 2005;26:2575–84. doi:10.1016/j.biomaterials.2004.07.041.
17. Barbara A, Delannoy P, Denis BG, et al. Normal matrix mineralization induced by strontium ranelate in MC3T3-E1 osteogenic cells. Metabolism. 2004;53:532–7. doi:10.1016/j.metabol.2003.10.022.
18. Marie PJ. Strontium ranelate: new insights into its dual mode of action. Bone. 2007;40:S5–8. doi:10.1016/j.bone.2007.02.003.
19. Caverzasio J. Strontium ranelate promotes osteoblastic cell replication through at least two different mechanisms. Bone. 2008;42:1131–6. doi:10.1016/j.bone.2008.02.010.
20. Wong CT, Chen QZ, Lu WW, et al. Ultrastructural study of mineralization of a strontium-containing hydroxyapatite (Sr-HA) cement in vivo. J Biomed Mater Res. 2004;70A:428–35. doi:10.1002/jbm.a.30097.
21. Wong CT, Lu WW, Chan WK, et al. In vivo cancellous bone remodeling on a strontium-containing hydroxyapatite (Sr-HA) bioactive cement. J Biomed Mater Res. 2004;68A:513–21. doi:10.1002/jbm.a.20089.
22. Ni GX, Lu WW, Xu B, et al. Interfacial behaviour of strontium-containing hydroxyapatite cement with cancellous and cortical bone. Biomaterials. 2006;27:5127–33. doi:10.1016/j.biomaterials.2006.05.030.
23. Verberckmoes SC, Debroe ME. Dose-dependent effects of strontium on osteoblast function and mineralization. Kidney Int. 2003;64:534–43. doi:10.1046/j.1523-1755.2003.00123.x.
24. Nielsen SP. The biological role of strontium. Bone. 2004;35:583–8. doi:10.1016/j.bone.2004.04.026.
25. Li YW, Leong JCY, Lu WW, et al. A novel injectable bioactive bone cement for spinal surgery: a developmental and preclinical study. J Biomed Mater Res. 2000;52:164–70. doi:10.1002/1097-4636(200010)52:1<164::AID-JBM21>3.0.CO;2-R
26. Guo D, Xu K, Zhao X, et al. Development of a strontium-containing hydroxyapatite bone cement. Biomaterials. 2005;26:4073–83. doi:10.1016/j.biomaterials.2004.10.032.
27. Landi E, Tampieri A, Celotti G, et al. Sr-substituted hydroxyapatites for osteoporotic bone replacement. Acta Biomater. 2007;3:961–9. doi:10.1016/j.actbio.2007.05.006.